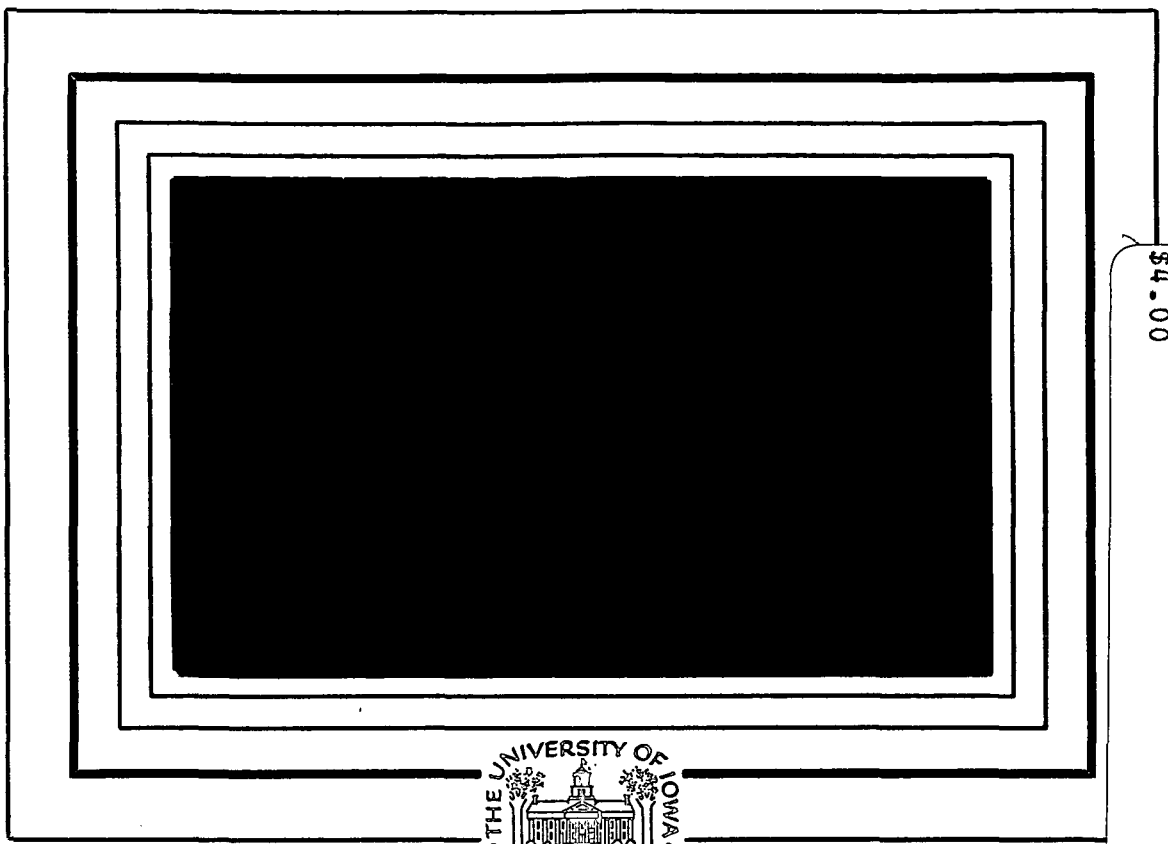

Research was sponsored in part by the Office of Naval Research under contract N00014-68-A-0196-0003.

Department of Physics and Astronomy
THE UNIVERSITY OF IOWA
Iowa City, Iowa

U. of Iowa/72:14

ELECTRIC FIELD AND PLASMA OBSERVATIONS IN THE MAGNETOSPHERE*+

by

Donald A. Gurnett

May 1972

Department of Physics and Astronomy
The University of Iowa
Iowa City, Iowa 52240

*Research supported in part by the National Aeronautics and Space Administration under contracts NAS5-10625, NAS1-8141, NAS1-2973, and grants NGL16-001-002, NGL16-001-043, and by the Office of Naval Research under contract N00014-68-A-0196-0003.

+To be presented as an invited paper at the 1972 COSPAR Symposium on Critical Problems of Magnetosphere Physics.

UNCLASSIFIED
Security Classification

DOCUMENT CONTROL DATA - R&D

(Security classification of title, body of abstract and indexing annotation must be entered when the overall report is classified)

1. ORIGINATING ACTIVITY *(Corporate author)*
Department of Physics and Astronomy
University of Iowa

2a. REPORT SECURITY CLASSIFICATION
UNCLASSIFIED

2b GROUP

3. REPORT TITLE
Electric Field and Plasma Observations in the Magnetosphere

4. DESCRIPTIVE NOTES *(Type of report and inclusive dates)*
Progress, May 1972

5. AUTHOR(S) *(Last name, first name, initial)*
Gurnett, Donald A.

6. REPORT DATE	7a. TOTAL NO. OF PAGES	7b. NO. OF REFS
May 1972	39	26

8a. CONTRACT OR GRANT NO.	9a. ORIGINATOR'S REPORT NUMBER(S)
N00014-68-A-0196-0003	U. of Iowa 72-14
b. PROJECT NO.	
c.	9b. OTHER REPORT NO(S) *(Any other numbers that may be assigned this report)*
d.	

10. AVAILABILITY/LIMITATION NOTICES
Approved for public release; distribution is unlimited.

11. SUPPLEMENTARY NOTES	12. SPONSORING MILITARY ACTIVITY
	Office of Naval Research

13. ABSTRACT

[See following page]

DD FORM 1 JAN 64 1473

UNCLASSIFIED
Security Classification

14. KEY WORDS	LINK A		LINK B		LINK C	
	ROLE	WT	ROLE	WT	ROLE	WT
Magnetospheric Electric Fields						
Electric Fields						

INSTRUCTIONS

1. ORIGINATING ACTIVITY: Enter the name and address of the contractor, subcontractor, grantee, Department of Defense activity or other organization *(corporate author)* issuing the report.

2*a*. REPORT SECURITY CLASSIFICATION: Enter the overall security classification of the report. Indicate whether "Restricted Data" is included. Marking is to be in accordance with appropriate security regulations.

2*b*. GROUP: Automatic downgrading is specified in DoD Directive 5200.10 and Armed Forces Industrial Manual. Enter the group number. Also, when applicable, show that optional markings have been used for Group 3 and Group 4 as authorized.

3. REPORT TITLE: Enter the complete report title in all capital letters. Titles in all cases should be unclassified. If a meaningful title cannot be selected without classification, show title classification in all capitals in parenthesis immediately following the title.

4. DESCRIPTIVE NOTES: If appropriate, enter the type of report, e.g., interim, progress, summary, annual, or final. Give the inclusive dates when a specific reporting period is covered.

5. AUTHOR(S): Enter the name(s) of author(s) as shown on or in the report. Enter last name, first name, middle initial. If military, show rank and branch of service. The name of the principal author is an absolute minimum requirement.

6. REPORT DATE: Enter the date of the report as day, month, year; or month, year. If more than one date appears on the report, use date of publication.

7*a*. TOTAL NUMBER OF PAGES: The total page count should follow normal pagination procedures, i.e., enter the number of pages containing information.

7*b*. NUMBER OF REFERENCES: Enter the total number of references cited in the report.

8*a*. CONTRACT OR GRANT NUMBER: If appropriate, enter the applicable number of the contract or grant under which the report was written.

8*b*, 8*c*, & 8*d*. PROJECT NUMBER: Enter the appropriate military department identification, such as project number, subproject number, system numbers, task number, etc.

9*a*. ORIGINATOR'S REPORT NUMBER(S): Enter the official report number by which the document will be identified and controlled by the originating activity. This number must be unique to this report.

9*b*. OTHER REPORT NUMBER(S): If the report has been assigned any other report numbers *(either by the originator or by the sponsor)*, also enter this number(s).

10. AVAILABILITY/LIMITATION NOTICES: Enter any limitations on further dissemination of the report, other than those imposed by security classification, using standard statements such as:

(1) "Qualified requesters may obtain copies of this report from DDC."

(2) "Foreign announcement and dissemination of this report by DDC is not authorized."

(3) "U. S. Government agencies may obtain copies of this report directly from DDC. Other qualified DDC users shall request through _____."

(4) "U. S. military agencies may obtain copies of this report directly from DDC. Other qualified users shall request through _____."

(5) "All distribution of this report is controlled. Qualified DDC users shall request through _____."

If the report has been furnished to the Office of Technical Services, Department of Commerce, for sale to the public, indicate this fact and enter the price, if known.

11. SUPPLEMENTARY NOTES: Use for additional explanatory notes.

12. SPONSORING MILITARY ACTIVITY: Enter the name of the departmental project office or laboratory sponsoring *(paying for)* the research and development. Include address.

13. ABSTRACT: Enter an abstract giving a brief and factual summary of the document indicative of the report, even though it may also appear elsewhere in the body of the technical report. If additional space is required, a continuation sheet shall be attached.

It is highly desirable that the abstract of classified reports be unclassified. Each paragraph of the abstract shall end with an indication of the military security classification of the information in the paragraph, represented as *(TS)*, *(S)*, *(C)*, *or (U)*.

There is no limitation on the length of the abstract. However, the suggested length is from 150 to 225 words.

14. KEY WORDS: Key words are technically meaningful terms or short phrases that characterize a report and may be used as index entries for cataloging the report. Key words must be selected so that no security classification is required. Identifiers, such as equipment model designation, trade name, military project code name, geographic location, may be used as key words but will be followed by an indication of technical context. The assignment of links, roles, and weights is optional.

ABSTRACT

Satellite-borne electric field measurements using the double probe technique have now provided a comprehensive survey of convection electric fields at low altitudes in the magnetosphere. The most prominent features of the convection electric fields are reversals located at high magnetic latitudes, with generally anti-sunward convection poleward and sunward convection equatorward of the electric field reversal location. The electric field reversal is usually coincident with the "trapping boundary" for electrons with energies $E > 45$ keV and is interpreted as the boundary between open and closed magnetic field lines. On the day side of the magnetosphere the electric field reversal is observed to coincide with the equatorward boundary of the polar cusp. In the local afternoon and evening regions "inverted V" electron precipitation bands occur at or near the electric field reversal and in regions usually characterized by large fluctuations in the electric field. In the local midnight region strong convection electric fields have also been observed deep within the magnetosphere, near the equatorward boundary of the plasma sheet. Recent measurements of electric fields near the "inverted V" electron precipitation bands suggests that these events are associated with large electrostatic potential gradients along the geomagnetic field.

I. INTRODUCTION

The importance of electric field measurements for studying the convective motions of plasma in the magnetosphere has been recognized for a number of years [Dungey, 1961; Axford and Hines, 1961; Piddington, 1962; Axford, 1969]. Only recently, however, have adequate techniques been developed to provide a comprehensive survey of electric fields in the magnetosphere. Electric field measurements with satellites [Cauffman and Gurnett, 1971; Heppner, 1972a] and ionized Barium cloud releases [Haerendel and Lust, 1970; Wescott et al., 1969] have now established the primary features of magnetospheric plasma convection at low altitudes over the auroral zones and polar caps. Since electric fields must ultimately be responsible for the acceleration and energization of charged particles in the magnetosphere, it is of great interest to determine the relationships between the electric fields and plasmas in the magnetosphere. Although extensive measurements of low-energy charged particles have been obtained [see the review by Hultquist, 1969, and the spatial survey by Frank and Ackerson, 1972] until recently the relationship between electric fields and charged particle intensities has been largely unexplored. In this paper we review the primary features of the electric field distribution over the auroral zones and polar caps as revealed by low-altitude polar orbiting satellites and discuss the relationship of these electric fields to the various plasma regiems of the magnetosphere as revealed by our current investigations.

II. SURVEY OF AURORAL ZONE AND POLAR CAP ELECTRIC FIELDS

Although numerous techniques, including Barium cloud releases and balloon-borne electric field measurements [Mozer and Serlin, 1969], have been employed in the measurement of auroral zone and polar cap electric fields, it is the recent advent of satellite measurements using the double-probe technique which has produced a comprehensive picture of these high-latitude electric fields. The first global survey of convection electric fields was obtained from the double-probe electric field experiment on the low-altitude (677 to 2528 km) polar orbiting satellite Injun 5 launched in August, 1968. Figure 1 from Cauffman and Gurnett [1971] shows a series of dawn-dusk passes over the northern polar region selected to illustrate the primary features of the high-latitude convection electric fields observed by Injun 5. The arrows in Figure 1 give the direction and magnitude of the convection velocity component measured, as computed from

$$\vec{V}_c = \frac{\vec{E}_c \times \vec{B}}{B^2} \quad ,$$

where $\vec{E}_c$ is the measured electric field (after subtracting the $\vec{V}\times\vec{B}$ field due to the spacecraft motion through the ionosphere) and $\vec{B}$ is the local geomagnetic field vector. Since only one component of the electric field was measured by Injun 5, only the components of the convection velocity indicated by the arrows could be determined on any single pass.

The most prominent and persistent feature of the Injun 5 electric field data is the occurrence of an abrupt reversal in the convection velocity and electric field at about 70° to 80° invariant latitude. These reversals are particularly evident in Figure 1 at about 1724:20, 1925:30 and 2123:30 UT in the dawn local time region and at 1734:00 and 2132:00 UT in the dusk local time region. In all cases, the reversals are consistent with a generally sunward flow on the equatorward side of the reversal and an anti-sunward flow on the poleward side of the reversal. The largest convection velocities are usually found within about 5° to 10° invariant latitude of the electric field reversal location. The convection velocities often exhibit a pronounced dawn-dusk asymmetry (evident in orbits 6910 and 6911 of Figure 1) with small, or near zero, convection velocities over a significant portion of the polar cap region. However, in some cases (such as orbit 6909 of Figure 1) the anti-sunward flow is nearly uniform along the entire satellite trajectory over the polar cap region. Only about 14% of the Injun 5 polar passes can be characterized as having uniform anti-sunward flow over the polar-cap region comparable to orbit 6909.

The OGO-6 satellite, launched in June 1969 into a low-altitude near polar orbit, also carried a double-probe electric field experiment [Heppner, 1972a] which shows many of the same features of the high-latitude convection revealed by Injun 5. The electric field for a series of dawn-dusk passes of OGO-6 over the northern hemisphere is shown in Figure 2 [these data were kindly provided by J. Heppner and T. Aggson]. The electric antenna axis during this series of passes is oriented

approximately perpendicular to the spacecraft-sun line so the electric field directly indicates the sunward (positive) and anti-sunward (negative) component of the plasma convection velocity. Electric field reversals are evident in both the dawn and dusk regions, separating the region of generally anti-sunward flow over the polar cap from the sunward flow at lower latitudes. These data clearly illustrate the large variability in the anti-sunward plasma flow over the polar region, ranging from nearly uniform flow (as in orbits 64, 83, and 121) to very asymmetrical flow patterns with large convection velocities near one of the reversals and near zero convection velocities on the opposite side of the polar region (as in orbits 130, 155, 184, 208, 222, 226, and 236).

Figures 1 and 2 illustrate the close similarity between the Injun 5 and OGO-6 convection electric field observations in the dawn-dusk meridional plane. Qualitatively both sets of data show (1) the persistent occurrence of electric field reversals at about 70° to 80° invariant latitude, (2) the occurrence of generally anti-sunward convection poleward of the electric field reversal and sunward convection equatorward of the electric field reversal, (3) the large variability in the profile of the anti-sunward plasma flow over the polar region, ranging from nearly uniform profiles in some cases to very asymmetrical profiles, with large differences between the dawn and dusk, in other cases. The only quantitative disagreement between these two sets of data appears to be in the relative occurrence and emphasis of the different types of anti-sunward convection profiles. Whereas the Injun 5 data show that cases of relatively uniform anti-sunward

convection over the polar region, such as orbit 6909 in Figure 1, are relatively uncommon (~ 14%) the examples shown by Heppner [1972a] give the impression that nearly uniform anti-sunward flow is the most common form of plasma flow over the polar region. Heppner [1972b] has recently emphasized that asymmetric convection profiles are also frequently observed in the OGO-6 data, as evident from Figure 2, and has established a relationship of these convection profiles with the direction of the interplanetary magnetic field.

The general features of the high-latitude electric fields at other local times have been obtained by Cauffman and Gurnett [1972] from a survey of all of the Injun 5 electric field data. The electric field reversals evident in the dawn-dusk passes of Figures 1 and 2 are a consistent feature of the high-latitude electric field data at all local times except in the local evening and local midnight regions. In these regions electric field reversals are also observed, however the electric field variations are usually more complex and variable, often consisting of multiple reversals and large fluctuations which cannot be simply identified as a single electric field reversal. The main features of the high-latitude convection pattern deduced from these data are summarized in Figure 3. The two diagrams of Figure 3 are intended to emphasize the variability of the convection pattern, from distinctly non-uniform anti-sunward flow over the polar cap region, as in (a), to nearly uniform anti-sunward flow over the polar cap region, as in (b). The dashed line in Figure 3, separating the regions of sunward

and anti-sunward flow, is the average location of the electric field reversal obtained from the Injun 5 data by Cauffman and Gurnett [1972]. It must be emphasized that these convection diagrams represent a gross average and the actual convection pattern may differ markedly from these "average" patterns. Major departures include:

(1) dawn-dusk asymmetries in the convection, usually consisting of marked differences in the size and intensity of the dawn and dusk convection cells,

(2) multiple reversals and irregular fluctuations, particularly in the local evening, possibly indicative of a turbulent eddy-like convection pattern in these regions,

(3) variations in the location of the "stagnation point" for the east-west plasma flow near local noon, and

(4) temporal variations in the latitude of the electric field reversal.

The anti-sunward convection over the polar region and the associated two-cell convection pattern inferred from these measurements provide strong evidence of the merging of the geomagnetic field lines with the interplanetary magnetic field as suggested by Dungey [1961]. Frank and Gurnett [1972] have shown that the electric field reversal corresponds to the boundary between "open" magnetic field lines, which connect into the solar wind, on the poleward side of the reversal and "closed" field lines, which connect to the opposite hemisphere without crossing the magnetopause, on the equatorward side of the reversal. An observational model which accounts for the nonuniform anti-sunward convection of magnetic field lines over the polar regions has been presented by Frank [1971a, b] and Frank and Gurnett [1971].

III. ELECTRIC FIELD REVERSALS AND THE ELECTRON E > 45 keV TRAPPING BOUNDARY

In an initial investigation of electric fields and their association with charged particle intensities Frank and Gurnett [1971] found that the "trapping boundary" for electrons with energies E > 45 keV is located essentially coincident with the electric field reversal. This relationship is illustrated in Figure 4, which shows the electric field and charged particle intensities for a dawn-dusk pass over the northern polar region. The electron E > 45 keV trapping boundary, which is observationally identified with the high-latitude termination of measurable E > 45 keV electron intensities, is shown by the vertical dashed lines at 1443 and 1453 UT. The electric field measurements obtained during this pass display a clearly defined electric field reversal, separating regions of sunward and anti-sunward convection, at about 1443 UT in the local dawn region and a less distinct reversal at 1453 UT in the local dusk region. The electric field reversal in the local dawn is seen to be located essentially coincident with the electron E > 45 keV trapping boundary. Examination of numerous other passes at other local times has shown that when an electric field reversal can be clearly identified, the electron E > 45 keV trapping boundary is almost always located essentially coincident with the electric field reversal. Since open magnetic field lines cannot sustain trapped energetic electron intensities, the observed

correspondence between the electron E > 45 keV trapping boundary and the electric field reversal provides further evidence that the electric field reversal corresponds with the boundary between open and closed magnetic field lines.

An unusual case in which the trapping boundary does not correspond with the location of the electric field reversal is shown in Figure 5. This pass occurred just preceding the expansion phase of a substorm [Gurnett and Frank, 1972b]. In the local evening region of this pass the electron E > 45 keV trapping boundary is located at about 1516:00 UT, several degrees equatorward of the electric field reversal at 1519:00 UT and in the zone of sunward convection. In this case we attribute the poleward movement of the electric field reversal, relative to its usual position near the trapping boundary, as being due to the rapid reconnection and creation of "new" closed field lines in the distant plasma sheet which are not yet populated by energetic (E > 45 keV) electrons. The region of sunward plasma flow in the local evening sector is also associated with the enhanced low-energy electron and proton intensities shown by the shaded band in Figure 12. From the relatively soft energy spectrums and overall intensities of these particles and their location on closed magnetic field lines, this region of low-energy electron and proton intensities has been identified with the plasma sheet along the evening flanks of the magnetosphere [Gurnett and Frank, 1972b]. This identification of plasma-sheet electrons and protons poleward of the trapping boundary and in the region of sunward convection (the shaded part of Figure 5) provides

substantial evidence of the increased reconnection rate and creation of new closed field lines in the plasma sheet during the initial phase of the substorm. One hour later, during the decay phase of the substorm, the electric field reversal is observed to have relaxed back to its usual position near the electron $E > 45$ keV trapping boundary.

IV. ELECTRIC FIELDS AND AURORAL PARTICLE PRECIPITATION

From the observations of Frank [1971a], it is known that plasma from the dayside magnetosheath has direct access into the high-latitude magnetosphere through a region called the polar cusp. Figure 6 illustrates a meridional pass by Injun 5 [Gurnett and Frank, 1972b] through the polar cusp region in the early-afternoon local time sector. The polar cusp region, encountered on this pass from about 0850:10 to 0852:10 UT, is easily identified by the enhanced intensities of low-energy electrons ($105 \leq E \leq 185$ eV) and protons ($290 \leq E \leq 455$ eV) shown shaded in Figure 6. The polar cusp region is located adjacent to and poleward of the electron $E > 45$ keV trapping boundary indicated by the vertical dashed line at about 0850:10 UT. The enhanced low-energy electron intensities occur in a narrow latitudinal band located essentially coincident with the electron $E > 45$ keV trapping boundary. The polar cusp proton fluxes occur in a somewhat broader zone extending several degrees invariant latitude poleward of the trapping boundary. The intense broad-band VLF hiss shown in the top panel of Figure 6 is believed to be generated by the low-energy ($\sim$ 100 eV) polar cusp electrons [Gurnett and Frank, 1972a]. The electric field measurements for this pass, in the second panel from the top in Figure 6, show a clearly defined electric field reversal at about 0850:10 UT, coincident with the electron $E > 45$ keV

trapping boundary and at the equatorward boundary of the polar cusp region. A polar diagram showing the convection velocity components associated with these electric field measurements is shown in Figure 7. The plasma convection in the polar cusp region is eastward and in a generally anti-sunward direction indicating that the polar cusp plasma is on "open" field lines which connect with the solar wind magnetic field through the dayside magnetosheath. The westward plasma flow equatorward of the electric field reversal, within the region of measurable electron $E > 45$ keV intensities, constitutes the return flow of plasma on closed field lines toward the dayside magnetopause.

Frank and Ackerson [1972] have shown that when the low-energy electron precipitation band in the polar cusp is followed around into the local evening, the average energy of the precipitated electrons increases to several keV or more. These electron precipitation bands have a characteristic "inverted V" energy-time signature in which the average electron energy increases to a maximum and subsequently decreases as the spacecraft passes through the precipitation region [Frank and Ackerson, 1971]. These "inverted V" electron precipitation bands have been directly associated with visible auroral arcs [Ackerson and Frank, 1972].

The precipitated electron energy flux associated with a series of "inverted V" events observed in the early local evening sector is shown in Figure 8. The most intense "inverted V" event on this pass was encountered from about 0027:45 to 0028:05 UT, as indicated by the large increase in the electron energy flux during this interval,

up to ~ 10 ergs $(cm^2\text{-sec-sr})^{-1}$. Color energy-time spectrograms which clearly show the "inverted V" characteristic of this event are being published separately [Gurnett and Frank, 1972b]. As is typical of these events [Frank and Ackerson, 1971], the "inverted V" electron precipitation band is located poleward of the electron $E > 45$ keV trapping boundary.

Frank and Gurnett [1971] have shown that "inverted V" electron precipitation events are closely associated with electric field reversals. This relationship is evident from the electric field data in Figure 8 which shows a highly structured discontinuity in the electric field, indicative of an electric field reversal, from about 0027:45 to 0028:05 UT. The location of this electric field reversal is seen to be essentially coincident with the location of the "inverted V" event observed on this pass. Other similar data showing the occurrence of "inverted V" events coincident with the electric field reversal have been presented by Frank and Gurnett [1971].

In the late evening and midnight local time regions, where electric field reversals are often not clearly distinguishable, the "inverted V" electron precipitation events still have a distinctive signature in the electric field data. An example of an "inverted V" event on a pass through the local midnight region is shown in Figure 9. A very distinct "inverted V" event with a maximum electron energy flux of about 20 ergs $(cm^2\text{-sec-sr})^{-1}$ occurred from about 0622:55 to 0623:25 UT and several less distinct "inverted V" events of lower energy flux occurred from 0623:25 to 0624:45 UT. The electron energy-

time spectrogram for this pass is shown in Figure 7 of Frank's [1972] paper for this symposium.

As can be seen from the top panel of Figure 9 the electric field in the neighborhood of the "inverted V" events is characterized by large, ~ 50 mV $(m)^{-1}$ irregular fluctuations on a time scale of a few seconds. The most striking feature of these electric field variations is the ~ 125 mV $(m)^{-1}$ south-eastward spike in the electric field at 0622:55 UT and the similar, but oppositely directed (north-westward) spike at 0623:50 UT. As indicated by the vertical guide lines in Figure 9, these spikes correspond very closely with the boundaries of the most intense "inverted V" event observed during this pass. Note that the energy flux of the "inverted V" event is not located symmetrically relative to the spatial configuration of these oppositely directed fields. Irregular fluctuation in the electric field, often consisting of distinct pairs of oppositely directed spikes as in Figure 9, are a persistent feature of all "inverted V" events observed with Injun 5. In many cases these irregular fluctuations provide such a distinctive "signature" that the location of the "inverted V" events could be determined with good reliability from the electric field measurement alone without prior reference to the plasma observations.

The broad region of somewhat lower electron energy flux from about 0624:45 to 0627:30 UT in Figure 9 has been identified as the plasma sheet by Gurnett and Frank [1972b] from electron energy spectrums and intensities characteristic of this region. Within the plasma sheet region the large irregular electric field fluctuations

associated with the "inverted V" event have disappeared and the electric field variations are relatively smooth. Near the equatorward boundary of the plasma sheet the electric field increases to about 65 mV $(m)^{-1}$ and abruptly decreases to near zero at the equatorward boundary of the plasma sheet, which also corresponds closely with the plasmapause location on this pass. Similar large convection electric fields have been observed deep within the magnetosphere on other passes in the local midnight region [Gurnett and Frank, 1972b] indicating that electric fields may be more important than previously thought for the transport, loss, and de-energization of plasma sheet particles penetrating into this region of the magnetosphere [see discussions by Vasylinunas, 1968; and Kennel, 1969].

V. ELECTRIC FIELDS AND VISUAL AURORA

Since electric field measurements are readily obtained from Barium cloud releases under conditions when auroral light emissions can be observed [Wescott et al., 1969; Haerendel and Lust, 1970], it is important to relate the charged particle/electric field measurements obtained via satellites to ground observations of visual aurora. Because of the difficulty in obtaining suitable simultaneous satellite and ground data, no direct comparison of satellite electric field measurements with auroral light emissions have yet been reported.

In attempting to relate auroral light emissions to the electric field and plasma observations obtained by Injun 5, it is important to recognize the distinction, made by Frank and Ackerson [1971, 1972], between the "inverted V" electron precipitation bands and the adjacent but equatorward precipitation from the plasma sheet. During magnetically quiescent periods the precipitated energy flux in the local evening is usually dominated by the "inverted V" bands (see Figures 8 and 9, for example). Ackerson and Frank [1972] clearly show that the "inverted V" bands produce visible auroral arcs. Although the precipitated energy flux from the "inverted V" bands is usually greater, the plasma sheet electron precipitation is also sufficiently intense to produce auroral light emission equatorward of the "inverted V" precipitation. During the expansion phase of a substorm the precipitated

energy flux from the plasma sheet increases considerably [Ackerson, 1972] and for these periods the dominant auroral light emission is probably from the plasma sheet region. Since the "inverted V" electron precipitation band is usually located near or slightly poleward of the electric field reversal and the plasma sheet precipitation occurs equatorward of the electric field reversal, it is clearly important to distinguish these two precipitation regions when analyzing associations with auroral light observations. At this time, it is not clear how, or whether, these precipitation regions can be identified from visual auroral observations alone.

VI. EVIDENCE OF PARALLEL ELECTRIC FIELDS

For several years [Alfven, 1958; Carlqvist and Bostrom, 1970] it has been believed that electric fields parallel to the geomagnetic field may be responsible for auroral charged particle acceleration. Although direct measurements of parallel electric fields have been reported [Mozer and Fahleson, 1970] the existence of these fields and their relationship to the auroral charged particle acceleration has been quite uncertain and speculative. The identification of "inverted V" electron energy-time spectra and the discovery of oppositely directed, spike-like electric fields at the boundaries of the "inverted V" events, as in Figure 9, provides us with convincing new evidence that parallel electric fields are responsible for the electron acceleration in these events. As commented by Frank and Gurnett [1971] the unique energy spectrum of the "inverted V" events and their anisotropic distribution of electron intensities downward along the magnetic field is in itself strongly suggestive of acceleration by an electrostatic potential gradient along the geomagnetic field. The "inverted V" energy-time variation is easily accounted for by a potential difference along the magnetic field which varies from near zero at the boundaries of the "inverted V" to a maximum at the peak of the "inverted V". Qualitatively, the resulting electrostatic potential contours within the "inverted V" region must be as shown in

Figure 10. The electrons in the "inverted V" events are believed to originate from the magnetosheath [Frank and Ackerson, 1971] with energies on the order of 100 eV. The spread in electron energies commonly observed for the "inverted V" events, indicated by the cross-hatching in Figure 10, is thought to be due to heating or scattering from plasma instabilities in the precipitated electron beam, and is possibly related to the intense VLF hiss emissions associated with these events [Gurnett and Frank, 1972a].

The oppositely-directed spikes in the electric field at the boundaries of the "inverted V", as in Figure 9, are readily explained by the electric fields which develop near the boundaries of the "inverted V" as shown in Figure 10. If the electric field is zero outside of the "inverted V" the potential from the spacecraft to the base of the acceleration region, Φ_s, can be obtained by integrating the $\vec{E}_\perp$ electric field component along the satellite trajectory. A rough estimate of this integral for the case shown in Figure 9 gives a maximum value for Φ_s of ~ 6 kV. Since the maximum electron energy of the "inverted V" is about 15 keV, it is evident that a significant portion of the electron acceleration must take place below the satellite, which was at an altitude of about 2400 km in this case. Because the "inverted V" electron precipitation events involve a significant current parallel to the geomagnetic field [Frank and Ackerson, 1971] it seems most likely that this field-aligned "Birkeland" current is an important factor in producing these potential gradients along the geomagnetic field. Whether the mechanism responsible for these field-aligned

potential gradients is a space-charge region of the type discussed by Carlqvist and Bostrom [1970] or an anomalous resistivity produced by a plasma instability, as discussed by Kindel and Kennel [1971], remains to be determined.

ACKNOWLEDGMENTS

This research was supported in part by the National Aeronautics and Space Administration under contracts NAS5-10625, NAS1-8141, NAS1-2973, and grants NGL16-001-002, NGL16-001-043, and by the Office of Naval Research under contract N00014-68-A-0196-0003.

REFERENCES

Ackerson, K. L., Observations of charged particle precipitation over the auroral zone during a magnetic substorm, Submitted for publication, J. Geophys. Res., 1972.

Ackerson, K. L., and L. A. Frank, Correlated satellite measurements of low-energy electron precipitation and ground-based observations of a visible auroral arc, J. Geophys. Res., 77, 1128, 1972.

Alfven, H., On the theory of magnetic storms and aurorae, Tellus, 10, 104, 1958.

Axford, W. I., Magnetospheric convection, Reviews of Geophys., 7, 421, 1969.

Axford, W. I., and C. O. Hines, A unifying theory of high-latitude geophysical phenomena and geomagnetic storms, Can. J. Phys., 39, 1433, 1961.

Carlqvist, P., and R. Bostrom, Space charge regions above the aurorae, J. Geophys. Res., 75, 7140, 1970.

Cauffman, D. P., and D. A. Gurnett, Double-probe measurements of convection electric fields with the Injun 5 satellite, J. Geophys. Res., 76, 6014, 1971.

Cauffman, D. P., and D. A. Gurnett, Satellite measurements of high-latitude convection electric fields, Accepted for publication, Space Sci. Rev., 11, 1972.

Dungey, J. W., Interplanetary magnetic field and auroral zones, Phys. Rev. Lett., 6, 47, 1961.

Frank, L. A., Plasma in the earth's polar magnetosphere, J. Geophys. Res., 76, 5202, 1971a.

Frank, L. A., Comments on a proposed magnetospheric model, J. Geophys. Res., 76, 2512, 1971b.

Frank, L. A., Plasma entry into the earth's magnetosphere, Paper B.2.1 of the 1972 COSPAR Symposium on Critical Problems of Magnetosphere Physics, Madrid, Spain, 1972.

Frank, L. A., and K. L. Ackerson, Observations of charged particle precipitation into the auroral zone, J. Geophys. Res., 76, 3612, 1971.

Frank, L. A., and K. L. Ackerson, Local-time survey of plasma at low altitudes over the auroral zones, in press, J. Geophys. Res., 1972.

Frank, L. A., and D. A. Gurnett, Distributions of plasmas and electric fields over the auroral zones and polar caps, J. Geophys. Res., 76, 6829, 1971.

Gurnett, D. A., and L. A. Frank, VLF hiss and related plasma observations in the polar magnetosphere, J. Geophys. Res., 77, 172, 1972a.

Gurnett, D. A., and L. A. Frank, Observed relationships between electric fields and auroral particle precipitation, submitted for publication, J. Geophys. Res., 1972b.

Haerendel, G., and R. Lust, Electric fields in the ionosphere and magnetosphere, Particles and Fields in the Magnetosphere, B. M. McCormac, ed., Reinhold Book Company (Dordrecht, Holland), 213, 1970.

Heppner, J. P., Electric field variations during substorms: OGO-6 measurements, Rep. X-645-72-10, Goddard Space Flight Center, Greenbelt, Md., 1972a.

Heppner, J. P., High-latitude electric fields, Trans. Am. Geophys. Union, 53(4), (title only), 360, 1972b.

Hultqvist, B., Auroras and polar substorms: Observations and theory, Rev. Geophys., 7, 129, 1969.

Kennel, C. F., Consequences of a magnetospheric plasma, Rev. Geophys. 7, 379, 1969.

Mozer, F. S., and U. V. Fahleson, Parallel and perpendicular electric fields in an aurora, Planet. Space Sci., 18, 1563, 1970.

Piddington, J. H., A hydromagnetic theory of geomagnetic storms and auroras, Planet. Space Sci., 9, 947, 1962.

Vasylinunas, V. M., A survey of low-energy electrons in the evening sector of the magnetosphere with OGO 1 and OGO 3, J. Geophys. Res., 73, 2839, 1968.

Wescott, E. M., J. D. Stolarik, and J. P. Heppner, Electric fields in the vicinity of auroral forms from motions of barium vapor releases, J. Geophys. Res., 74, 3469, 1969.

FIGURE CAPTIONS

Figure 1 The convection velocity components determined for a series of dawn-dusk orbits of Injun 5 over the northern hemisphere. Note the persistent occurrence of electric field reversals at about 70° to 80° invariant latitude separating the anti-sunward plasma flow poleward of the reversal from the sunward flow at lower latitudes.

Figure 2 The dawn-dusk electric field observed for a sequence of dawn-dusk orbits of OGO-6 over the northern hemisphere. Note the occurrence of both uniform and asymmetrical anti-sunward convection profile over the polar region.

Figure 3 Schematic diagram showing "average" convection patterns observed by Injun 5 and OGO-6, ranging from (a) distinctly non-uniform and often asymmetrical anti-sunward flow over the polar region to (b) essentially uniform anti-sunward flow over the entire polar cap.

Figure 4 Simultaneous electric field and charged particle measurements showing the correspondence between the electric field reversals at 1443 and 1453 UT and the electron $E > 45$ keV trapping boundary (vertical dashed lines).

Figure 5 An unusual case during the initial phase of a substorm in which the electric field reversal at 1519 UT is located several degrees poleward of the electron E > 45 keV trapping boundary at 1516 UT.

Figure 6 Simultaneous observations of VLF hiss, convection electric fields, and charged particle intensities for a noon-midnight meridional pass over the southern polar cap and auroral zone. Note that the polar cusp is located in the zone of eastward convection just poleward of the electric field reversal and the electron (E > 45 keV) trapping boundary (see Figure 7).

Figure 7 A polar diagram showing the direction and magnitude of the convection velocity components associated with the electric field observations in Figure 6.

Figure 8 An early-evening pass showing a series of "inverted V" electron precipitation events located coincident with the electric field reversal at about 0027:45 to 0028:05 UT.

Figure 9 A pass near local midnight showing oppositely directed "spikes" in the electric field at the boundaries of the "inverted V" event from 0622:55 to 0623:50 UT and a large zone of plasma convection near the equatorward boundary of the plasma sheet.

Figure 10 Qualitative form of the electrostatic potential contours associated with an "inverted V" electron precipitation event. Note the oppositely directed $\vec{E}_{\perp}$ electric field at the boundaries of the "inverted V", similar to the case shown in Figure 9.

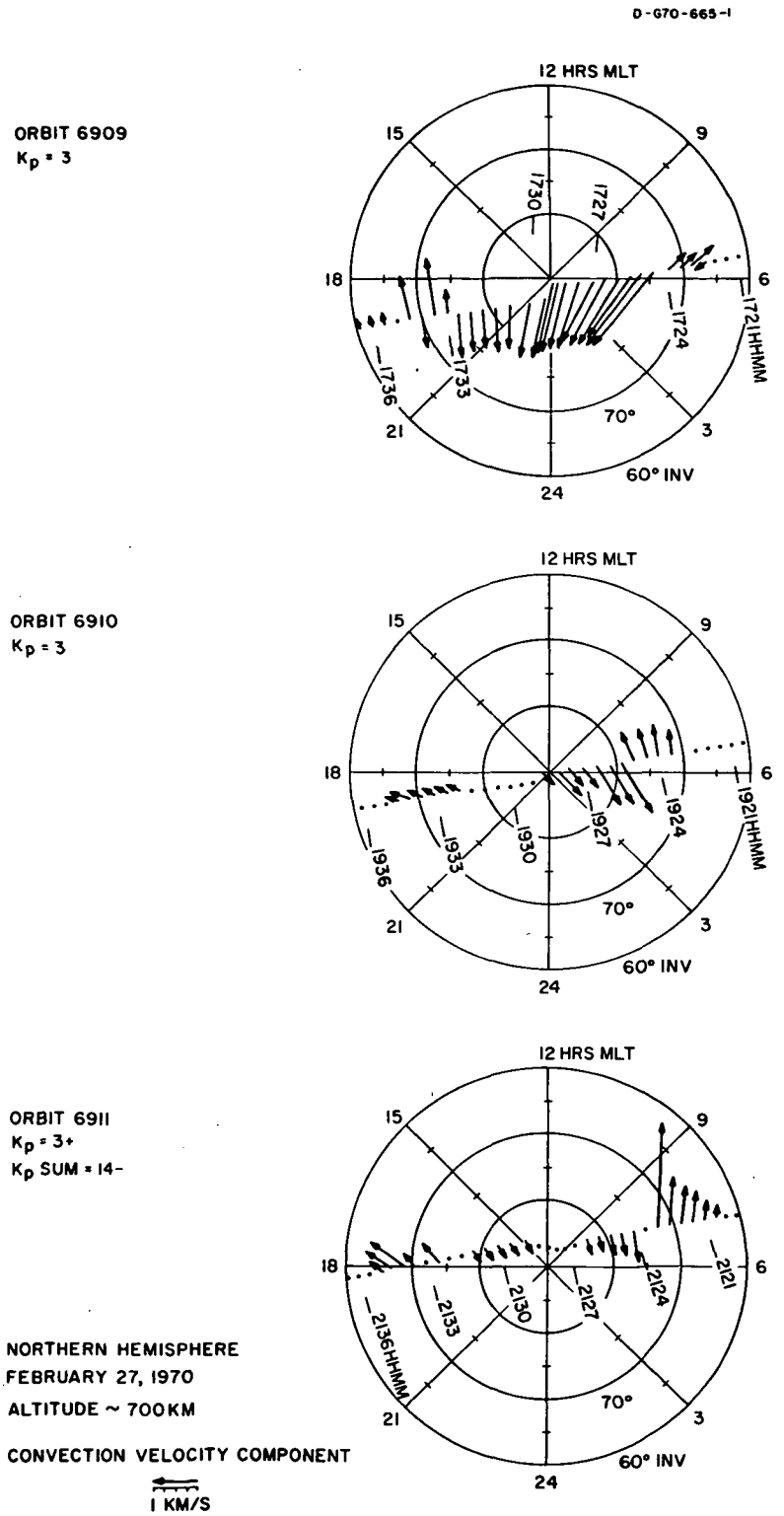
D-G70-665-1
ORBIT 6909
K_p = 3
12 HRS MLT
15
9
18
6
21
3
24
70°
60° INV
1730
1727
1724
1721HHMM
1733
1736
ORBIT 6910
K_p = 3
12 HRS MLT
1930
1927
1924
1921HHMM
1933
1936
ORBIT 6911
K_p = 3+
K_p SUM = 14-
12 HRS MLT
2130
2127
2124
2121
2133
2136HHMM
NORTHERN HEMISPHERE
FEBRUARY 27, 1970
ALTITUDE ~ 700KM
CONVECTION VELOCITY COMPONENT
1 KM/S

Figure 1

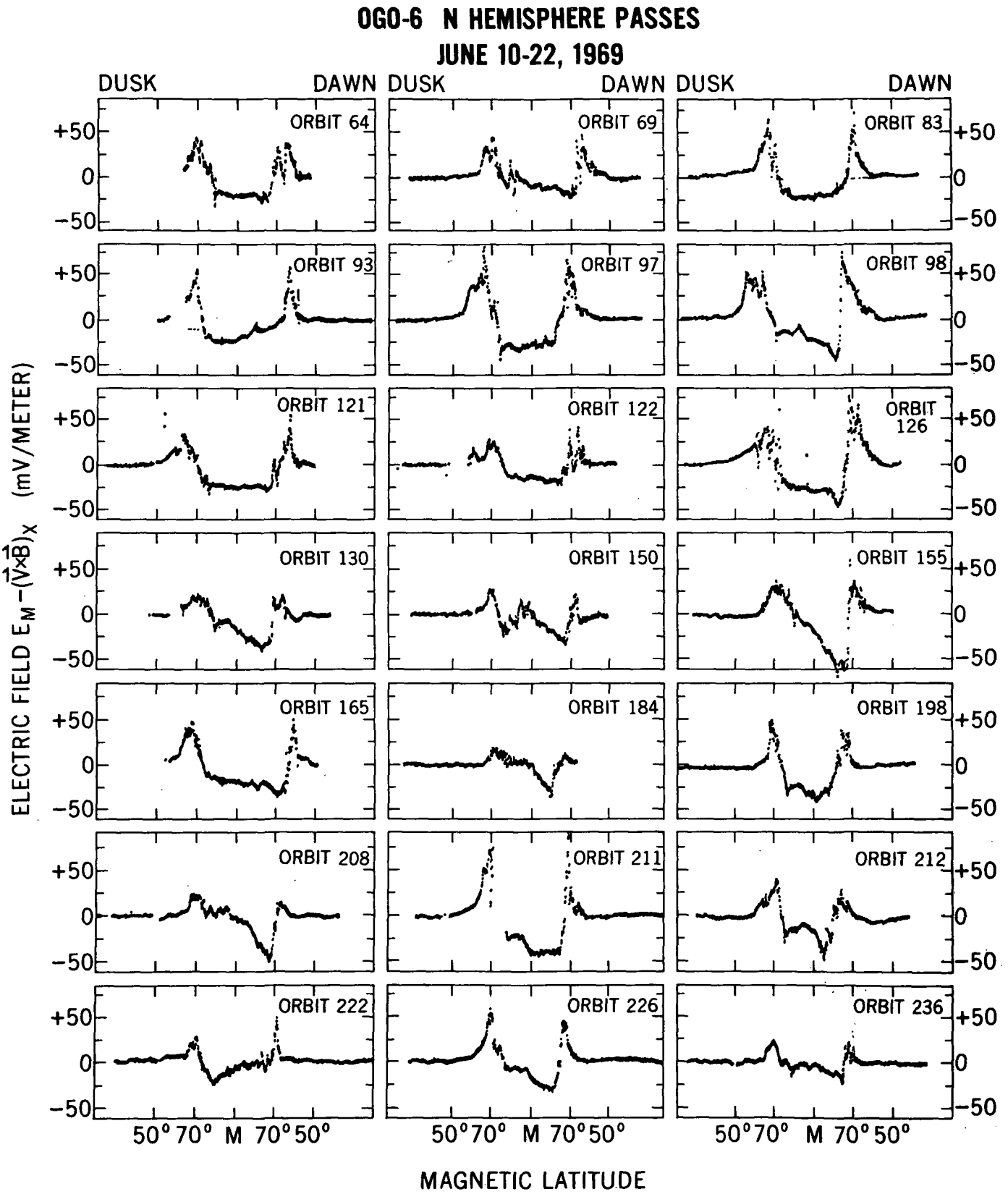
OGO-6 N HEMISPHERE PASSES
JUNE 10-22, 1969
DUSK
DAWN
ORBIT 64
ORBIT 69
ORBIT 83
ORBIT 93
ORBIT 97
ORBIT 98
ORBIT 121
ORBIT 122
ORBIT 126
ORBIT 130
ORBIT 150
ORBIT 155
ORBIT 165
ORBIT 184
ORBIT 198
ORBIT 208
ORBIT 211
ORBIT 212
ORBIT 222
ORBIT 226
ORBIT 236
+50
0
−50
50° 70° M 70° 50°
MAGNETIC LATITUDE
ELECTRIC FIELD $E_M - (\vec{V}\times\vec{B})_X$ (mV/METER)

Figure 2

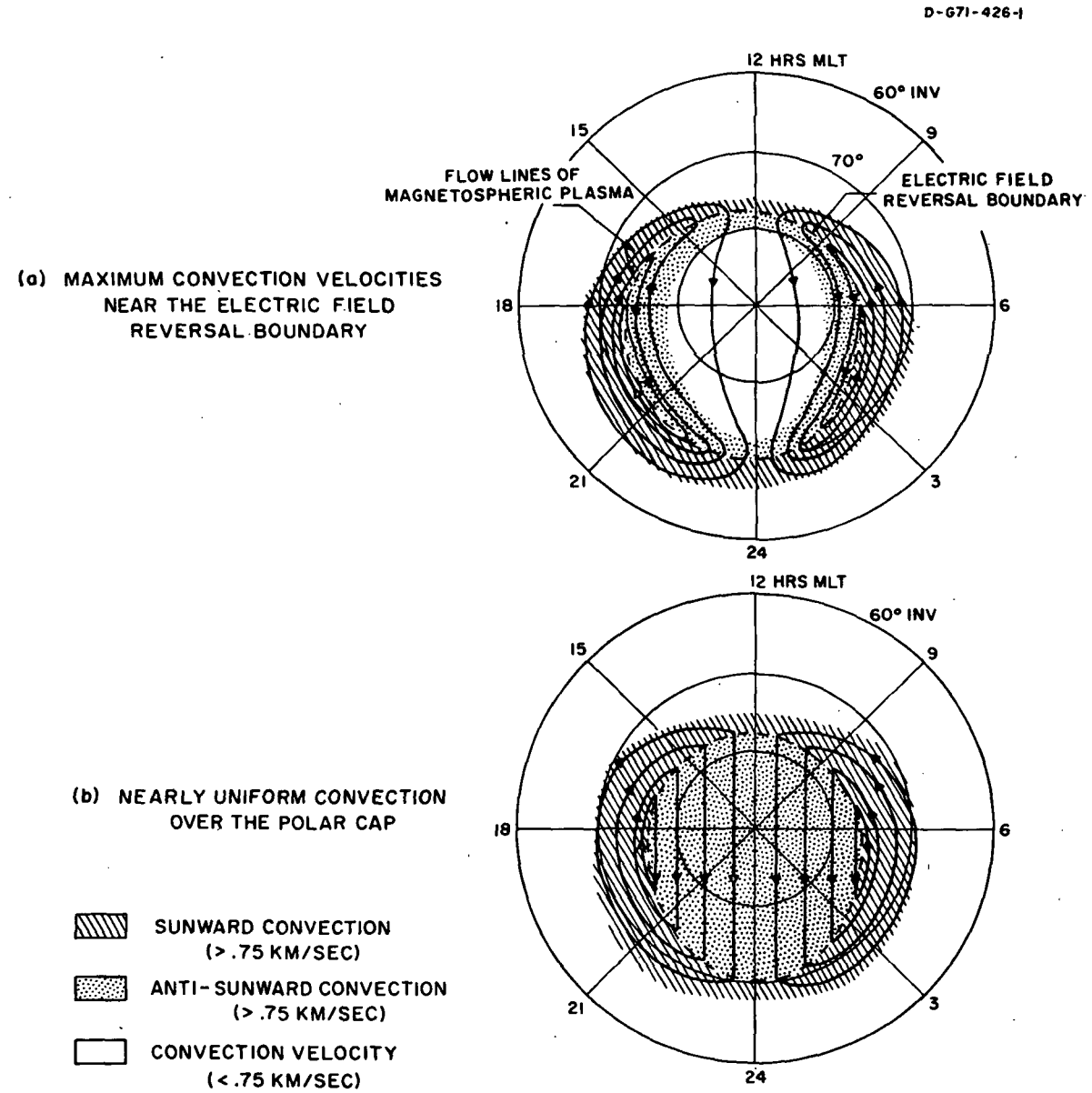
D-G71-426-1
12 HRS MLT
60° INV
15
9
70°
FLOW LINES OF
MAGNETOSPHERIC PLASMA
ELECTRIC FIELD
REVERSAL BOUNDARY
18
6
21
3
24
(a) MAXIMUM CONVECTION VELOCITIES
NEAR THE ELECTRIC FIELD
REVERSAL BOUNDARY
12 HRS MLT
60° INV
15
9
18
6
21
3
24
(b) NEARLY UNIFORM CONVECTION
OVER THE POLAR CAP
SUNWARD CONVECTION
(> .75 KM/SEC)
ANTI-SUNWARD CONVECTION
(> .75 KM/SEC)
CONVECTION VELOCITY
(< .75 KM/SEC)

Figure 3

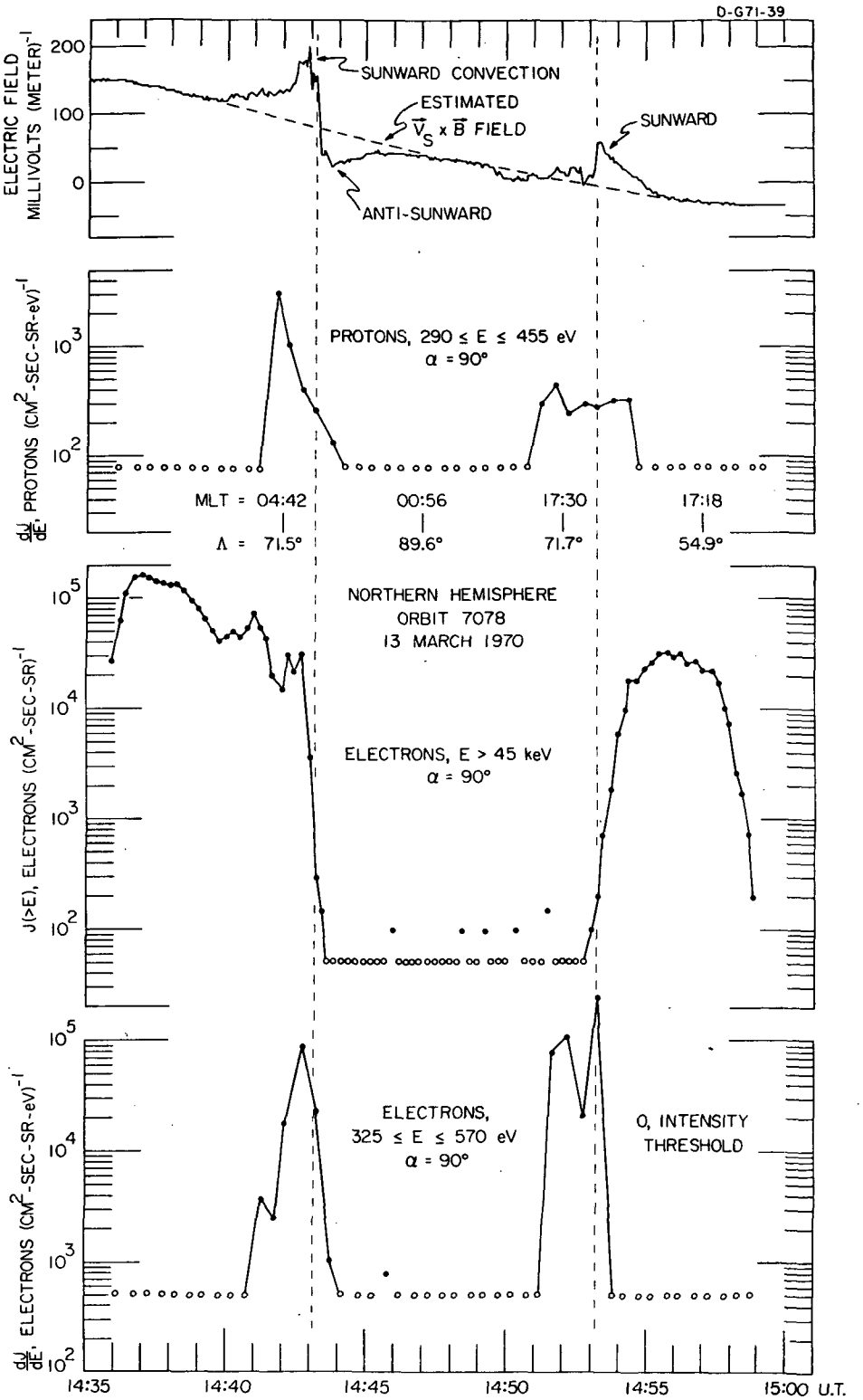
D-G71-39
ELECTRIC FIELD MILLIVOLTS (METER)$^{-1}$
200
100
0
SUNWARD CONVECTION
ESTIMATED
$\vec{V}_S \times \vec{B}$ FIELD
SUNWARD
ANTI-SUNWARD
$\frac{dJ}{dE}$, PROTONS (CM^2-SEC-SR-eV)$^{-1}$
10^3
10^2
PROTONS, 290 ≤ E ≤ 455 eV
α = 90°
MLT = 04:42
Λ = 71.5°
00:56
89.6°
17:30
71.7°
17:18
54.9°
J(>E), ELECTRONS (CM^2-SEC-SR)$^{-1}$
10^5
10^4
10^3
10^2
NORTHERN HEMISPHERE
ORBIT 7078
13 MARCH 1970
ELECTRONS, E > 45 keV
α = 90°
$\frac{dJ}{dE}$, ELECTRONS (CM^2-SEC-SR-eV)$^{-1}$
10^5
10^4
10^3
10^2
ELECTRONS,
325 ≤ E ≤ 570 eV
α = 90°
0, INTENSITY
THRESHOLD
14:35
14:40
14:45
14:50
14:55
15:00 U.T.

Figure 4

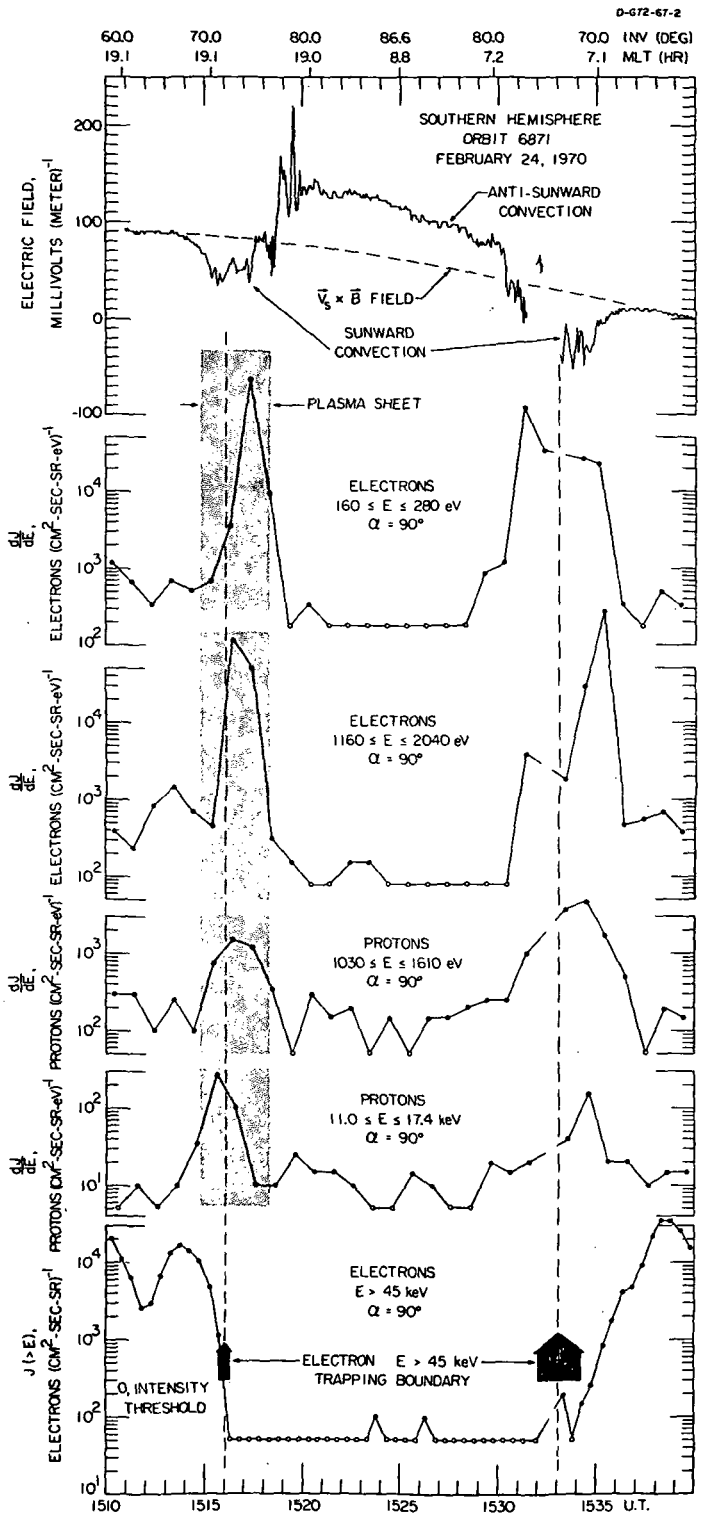
D-G72-67-2
60.0 70.0 80.0 86.6 80.0 70.0 INV (DEG)
19.1 19.1 19.0 8.8 7.2 7.1 MLT (HR)
SOUTHERN HEMISPHERE
ORBIT 6871
FEBRUARY 24, 1970
ANTI-SUNWARD CONVECTION
$\vec{V}_s \times \vec{B}$ FIELD
SUNWARD CONVECTION
ELECTRIC FIELD, MILLIVOLTS (METER)$^{-1}$
PLASMA SHEET
ELECTRONS 160 ≤ E ≤ 280 eV α = 90°
ELECTRONS 1160 ≤ E ≤ 2040 eV α = 90°
PROTONS 1030 ≤ E ≤ 1610 eV α = 90°
PROTONS 11.0 ≤ E ≤ 17.4 keV α = 90°
ELECTRONS E > 45 keV α = 90°
ELECTRON E > 45 keV TRAPPING BOUNDARY
0, INTENSITY THRESHOLD
1510 1515 1520 1525 1530 1535 U.T.

Figure 5

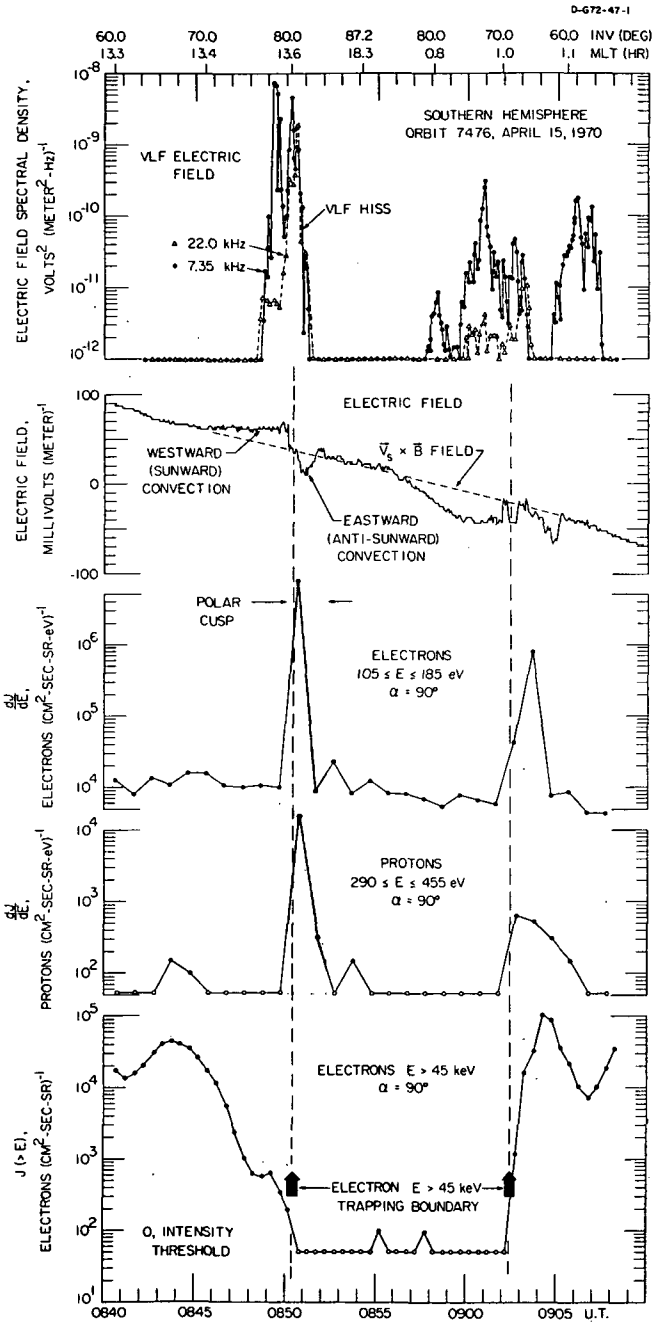
D-672-47-1
60.0 13.3
70.0 13.4
80.0 13.6
87.2 18.3
80.0 0.8
70.0 1.0
60.0 1.1 INV (DEG) MLT (HR)
SOUTHERN HEMISPHERE
ORBIT 7476, APRIL 15, 1970
VLF ELECTRIC FIELD
VLF HISS
▲ 22.0 kHz
• 7.35 kHz
ELECTRIC FIELD SPECTRAL DENSITY, VOLTS² (METER²-Hz)⁻¹
ELECTRIC FIELD
WESTWARD (SUNWARD) CONVECTION
$\vec{V}_s \times \vec{B}$ FIELD
EASTWARD (ANTI-SUNWARD) CONVECTION
ELECTRIC FIELD, MILLIVOLTS (METER)⁻¹
POLAR CUSP
ELECTRONS 105 ≤ E ≤ 185 eV α = 90°
ELECTRONS (CM²-SEC-SR-eV)⁻¹
PROTONS 290 ≤ E ≤ 455 eV α = 90°
PROTONS (CM²-SEC-SR-eV)⁻¹
ELECTRONS E > 45 keV α = 90°
ELECTRON E > 45 keV TRAPPING BOUNDARY
O, INTENSITY THRESHOLD
J (> E), ELECTRONS (CM²-SEC-SR)⁻¹
0840 0845 0850 0855 0900 0905 U.T.

Figure 6

SOUTHERN HEMISPHERE
ORBIT 7476
APRIL 15, 1970

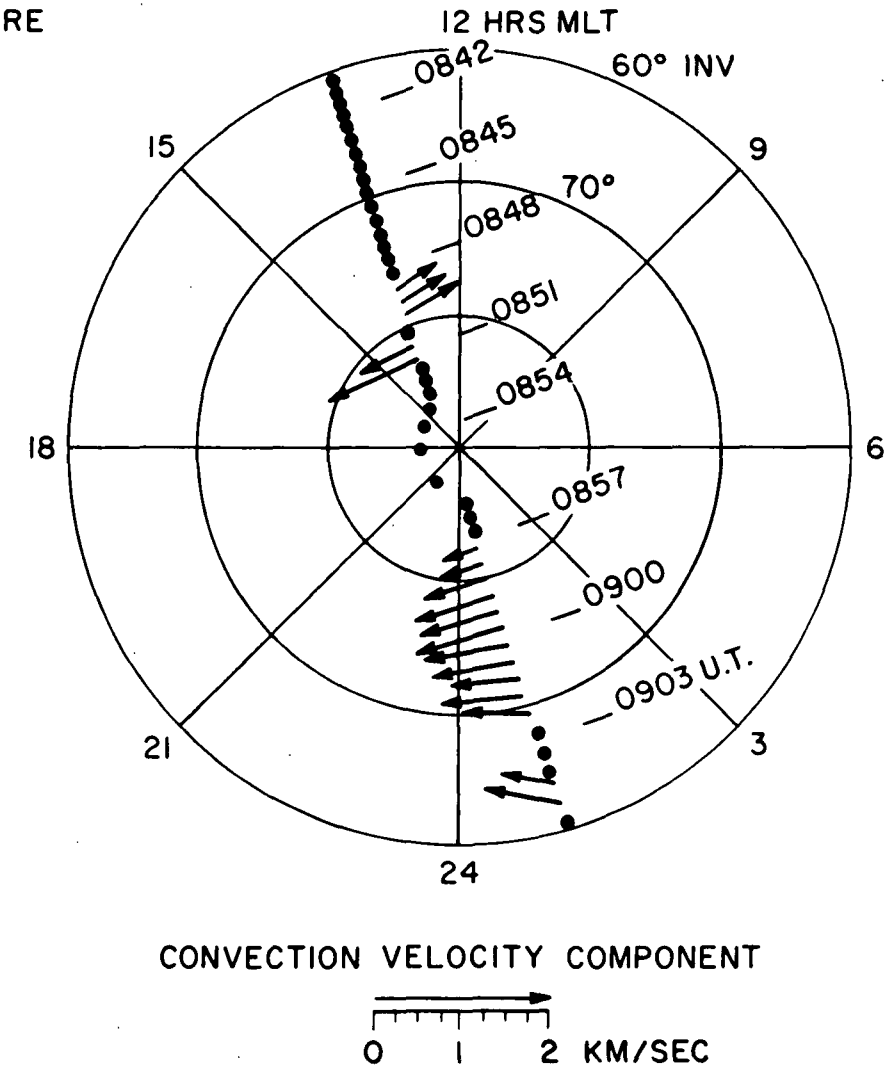

Figure 7

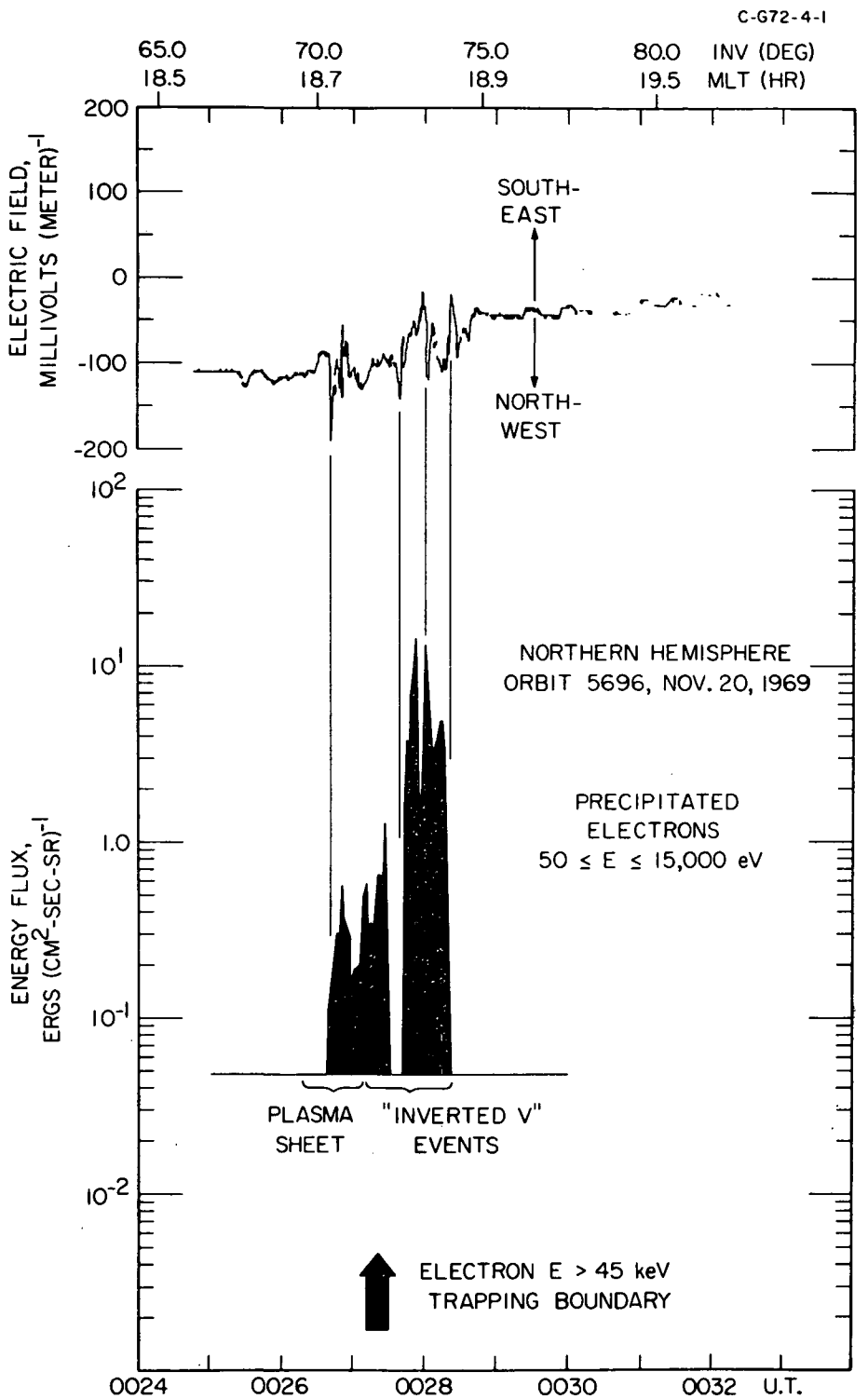
C-G72-4-1
65.0
18.5
70.0
18.7
75.0
18.9
80.0
19.5
INV (DEG)
MLT (HR)
ELECTRIC FIELD, MILLIVOLTS (METER)$^{-1}$
200
100
0
-100
-200
SOUTH-EAST
NORTH-WEST
10^2
10^1
1.0
10^{-1}
10^{-2}
ENERGY FLUX, ERGS (CM^2-SEC-SR)$^{-1}$
NORTHERN HEMISPHERE
ORBIT 5696, NOV. 20, 1969
PRECIPITATED ELECTRONS
50 ≤ E ≤ 15,000 eV
PLASMA SHEET
"INVERTED V" EVENTS
ELECTRON E > 45 keV
TRAPPING BOUNDARY
0024
0026
0028
0030
0032
U.T.

Figure 8

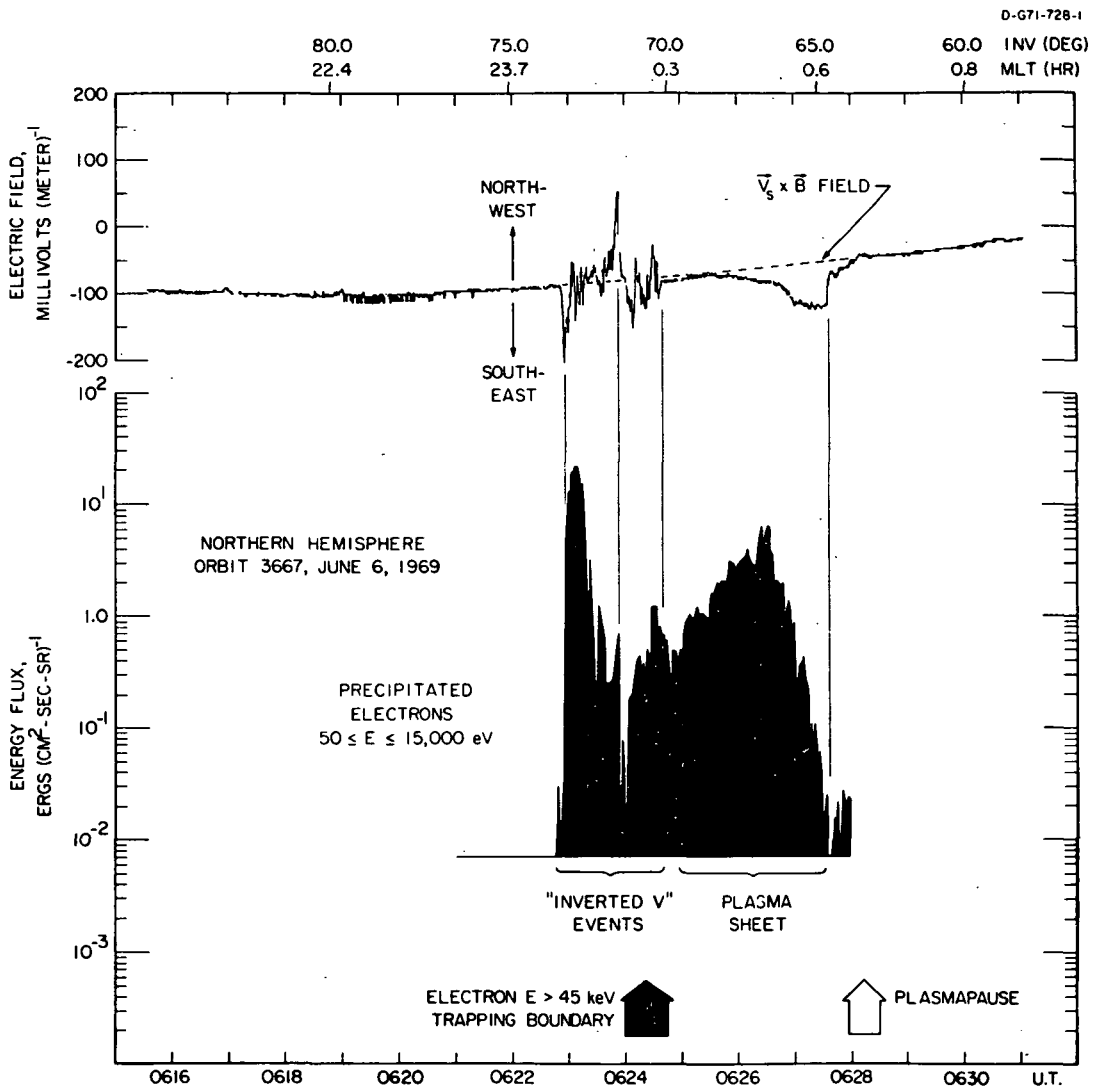
D-G71-728-1
80.0
22.4
75.0
23.7
70.0
0.3
65.0
0.6
60.0
0.8
INV (DEG)
MLT (HR)
ELECTRIC FIELD, MILLIVOLTS (METER)$^{-1}$
200
100
0
-100
-200
NORTH-WEST
SOUTH-EAST
$\vec{V}_s \times \vec{B}$ FIELD
NORTHERN HEMISPHERE
ORBIT 3667, JUNE 6, 1969
PRECIPITATED ELECTRONS
50 ≤ E ≤ 15,000 eV
ENERGY FLUX, ERGS (CM^2-SEC-SR)$^{-1}$
10^2
10^1
1.0
10^{-1}
10^{-2}
10^{-3}
"INVERTED V" EVENTS
PLASMA SHEET
ELECTRON E > 45 keV TRAPPING BOUNDARY
PLASMAPAUSE
0616
0618
0620
0622
0624
0626
0628
0630
U.T.

Figure 9

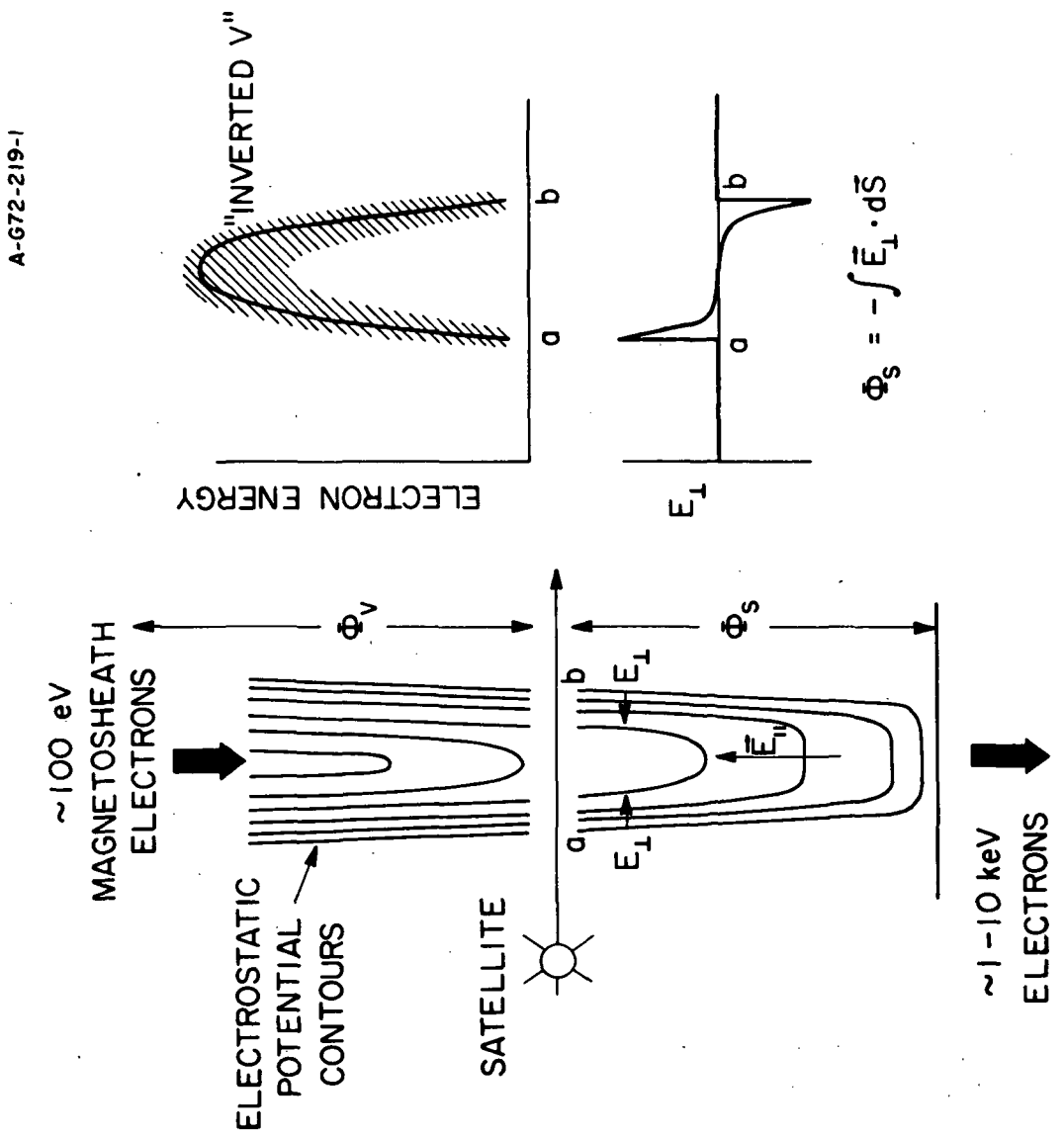
A-G72-219-I
"INVERTED V"
ELECTRON ENERGY
a
b
$E_\perp$
$\Phi_s = -\int \vec{E}_\perp \cdot d\vec{S}$
~100 eV
MAGNETOSHEATH
ELECTRONS
Φ_v
Φ_s
ELECTROSTATIC
POTENTIAL
CONTOURS
SATELLITE
$\vec{E}_\parallel$
~1-10 keV
ELECTRONS

Figure 10